REVIEW ARTICLE

The surprising Crab pulsar and its nebula: A review

R. Bühler[1], R. Blandford[2]

[1]Deutsches Elektronen Synchrotron DESY, D-15738 Zeuthen, Germany
[2]Kavli Institute for Particle Astrophysics and Cosmology, Department of Physics and SLAC National Accelerator Laboratory, Stanford University, Stanford, CA 94305, USA

E-mail: `rolf.buehler@desy.de, rdb@slac.stanford.edu`

Abstract. The Crab nebula and its pulsar (referred to together as "Crab") have historically played a central role in astrophysics. True to their legacy, several unique discoveries have been made recently. The Crab was found to emit gamma-ray pulsations up to energies of 400 GeV, beyond what was previously expected from pulsars. Strong gamma-ray flares, of durations of a few days were discovered from within the nebula, while the source was previously expected to be stable in flux on these time scales. Here we review these intriguing and suggestive developments. In this context we give an overview of the observational properties of the Crab and our current understanding of pulsars and their nebulae.

PACS numbers: 97.60.Bw, 97.60.Gb, 97.60.Jd

Contents

1. Introduction

On August 25, 1054 A.D., the Chinese astrologer Yang Wêlt reported "the appearance of a guest star, above which some yellow-colored light was faintly seen". He goes on to interpret the observations as showing that "there is a person of great wisdom and virtue in the country. I beg that the Bureau of Historiography be given this message"‡ (Peng-Yoke et al. 1972). Yang Wêlt's message was heard and today we know that the new star which emerged in July 1054 A.D. on the night sky was the Crab supernova (Breen & McCarthy 1995). Since then the remainder of this explosion, the Crab nebula and its pulsar, has been studied over the centuries. The source was rediscovered by an English amateur John Bevis who included it in a beautiful atlas which was never published because the publishers went bankrupt. He told his French colleague, Charles Messier about it. Messier was more interested in comets, to him the Crab Nebula was noise not signal. He included it in a famous catalog of celestial objects that could be confused with comets. The Crab is the first entry. The name of the nebula is due to an Irishman, the third Earl of Rosse, who thought it looked like a Crab.

Following observations from J C Duncan in 1921, Edwin Hubble noted that, not only the Universe, but also the Crab nebula is expanding (Hubble 1928). From the expansion velocity he correctly deduced that the nebula was the remainder of the 1054 A.D. star explosion, making the Crab the first historical supernova. In one of the most celebrated and concise conjectures in the history of astronomy, Baade and Zwicky in 1934 "advanced the view" that in a supernova "mass in bulk is annihilated", "cosmic rays are produced" and that they "represent a transition from ordinary stars into neutron stars" (Baade & Zwicky 1934). In 1942, Minkowski correctly associated one of the two central stars in the nebula with the explosion and in 1967 Pacini proposed that this star was a highly magnetized, spinning neutron star and that it powered the nebula (Pacini 1967). The idea was put on a firmer footing by Gold who equated the rate of loss of rotational energy by the neutron star with the bolometric luminosity of the nebula (Gold 1968). Almost 1000 years after the explosion of the progenitor star, the Crab is far from being quiet. At photon energies above $\gtrsim 30$ keV, it is typically one of the brightest sources in the sky.

Due to its high luminosity $L \approx 1.3 \times 10^{38}$ erg s^{-1} (Hester 2008) and its proximity of ~ 2 kpc (Trimble 1973), the Crab can be studied in great detail. It is therefore one of our prime laboratories to study non-thermal processes in the Universe. Many discoveries have been made in the Crab and then been seen in other non-thermal sources (including active galactic nuclei, gamma ray bursts and X-ray binaries) such as polarized synchrotron radiation or pulsed optical emission (Shklovsky 1953, Cocke et al. 1969). True to this legacy two remarkable discoveries have been made in the last years. Very high-energy (VHE $\gtrsim 100$ GeV) gamma-ray emission has been detected from the pulsar, and high-energy (HE $\gtrsim 100$ MeV) gamma-ray flares have been discovered from the

‡ The term "guest star" was used by Chinese astronomers for new stars in the night sky, as novae or supernovae.

nebula. These phenomena have not been observed in any other pulsar wind nebula to date. As we will discuss, they challenge and extend our understanding of these systems.

This article is structured as follows: first we will summarize the observational properties of the Crab and our current theoretical understanding of pulsar wind nebulae (section 2 & 3). We will proceed to discuss the discovered gamma-ray pulsations and flares together with the ideas put forward so far to explain them (section 4 & 5). Finally, we conclude the article with an outlook on future observational and theoretical developments. We would like to note that, given the wealth of work done on this source, it is not possible for us to be exhaustive. We will therefore give references to related review articles whenever possible. A more detailed description of the observational properties of the Crab can for instance be found in Hester (2008). A more detailed discussion of the theory of pulsar wind nebulae can be found in Kirk & Lyubarsky (2009) and Arons (2012).

2. Observational overview

The Crab nebula can be seen in a composite image in Fig. 1. The point source at its center is the Crab pulsar, the energy source of the system (see Rowan & Coontz (2004) and Harding (2013) for reviews on neutron stars and pulsars). Its energy is in its largest part emitted in a relativistic flow of magnetized plasma. This pulsar wind is thought to be predominantly composed of electron-positron pairs (referred to together as electrons in the following), although some ions might be present (Gallant & Arons 1994). These pairs flow outwards and interact with the remaining ejecta of the progenitor star. As these particles spread out in the nebula, they loose energy due to synchrotron and inverse Compton radiation, creating the glowing pulsar wind nebula observed today. In the following we will describe the observations of the pulsar and the nebulae in more detail.

2.1. The Crab pulsar

The pulsar emits radiation across the electromagnetic spectrum with a period of $P_{\mathrm{Crab}} = 33.6$ ms, which is slowing down by $\dot{P}_{\mathrm{Crab}} = 4.2 \times 10^{-13}$ (Manchester et al. 2005, Abdo et al. 2013). The corresponding loss of rotational energy is $\dot{E} \approx 5 \times 10^{38}$ erg s^{-1}, assuming a moment of inertia of the neutron star of $I \approx 10^{45}$ g cm^{-2}. Only $\sim 1\%$ of this energy is emitted in electromagnetic radiation. The radiation is thought to be collimated in beams of light, which sweep the field of view of the Earth, creating the observed pulsations. The phase-averaged spectral energy distribution (SED) is shown in Fig. 2. It is composed of three main components: the first one in the radio band, a second energetically dominant component peaking in the X-ray band and a third one emerging above energies of ~ 100 MeV.

The phase profile of the emission is shown in Fig. 3. As for the majority of pulsars detected in gamma rays by the Fermi Large Area Telescope (LAT), the radiation as

Figure 1. A composite image of the Crab Nebula showing X-ray in blue, optical in green, and radio in red. The angular size of the image on the sky is 7.9 arc minutes on each side (Hester 2013). Credits: X-ray: NASA/CXC/ASU/J. Hester et al.; Optical: NASA/HST/ASU/J. Hester et al.; Radio: NRAO/AUI/NSF. The white box indicates the region shown in Fig. 4.

a function of phase ϕ is concentrated in two peaks (Abdo et al. 2013). The pulses arrive approximately simultaneously across the electromagnetic spectrum, only small shifts between energy bands are seen ($\Delta\phi \lesssim 0.01$; Oosterbroek et al. (2008) and Abdo et al. (2010)). The main pulse $P1$ is located at $\phi \approx 1.0$ and the inter-pulse $P2$ at $\phi \approx 0.4$. A faint precursor to $P1$ is detected at radio frequencies, and at frequencies above the optical bridge emission is found between $P1$ and $P2$. A peculiarity of the pulse profile of the Crab is that it is unusually irregular on short time scales. Giant radio pulses with a flux 1000 times the average are seen randomly during $P1$ and $P2$ (Lundgren et al. 1995, Cordes et al. 2004, Popov & Stappers 2007). Optical emission was seen to increase during such events (Shearer et al. 2003, Strader et al. 2013), but no such correlation has been found so far with higher energies (Bilous et al. 2011, Bilous et al. 2012, Aliu et al. 2012). Pulsar glitches, during which for a limited time the spin-down frequency increases by up to $\sim 10^{-5}$ Hz, are observed ~ 1 per year (Lyne et al. 1993, Espinoza et al. 2011, Wang et al. 2012).

The pulsar emission is found to be polarized. The position angle PA of the linearly polarized component varies with pulse phase. The polarization properties in radio depend on frequency. Generally, the polarization degree and angle vary smoothly, with no abrupt changes during the main pulses (Moffett et al. 1999). The Crab is one of the few pulsars for which polarization has also been detected at optical wavelength (Slowikowska et al. 2009, Moran et al. 2013). The optical polarization angle swings from $PA \approx 40°$ to $PA \approx 170°$ during P1, decreases again during the bridge emission
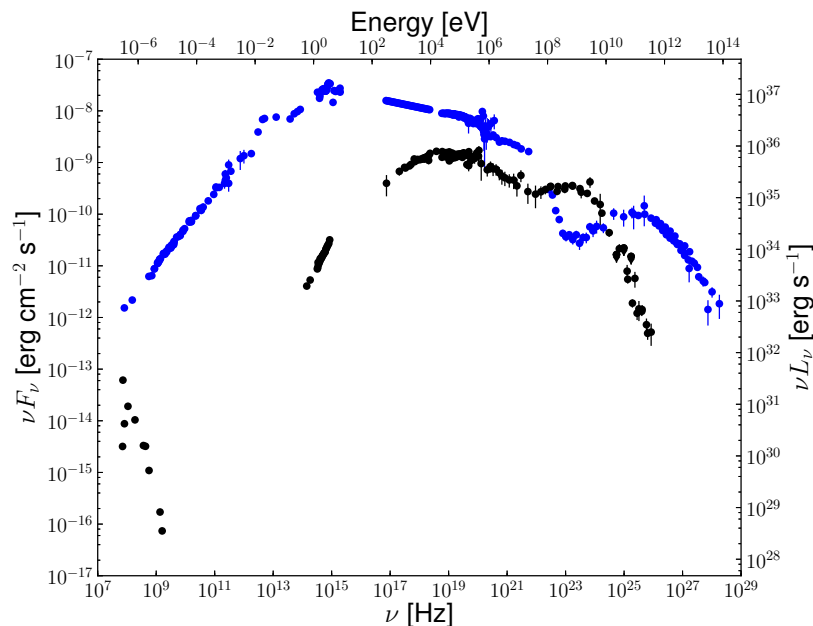
Figure 2. Spectral energy distribution of the average emission of the Crab nebula (blue) and the phase averaged emission of the Crab pulsar (black). The data for the nebula were taken from Meyer et al. (2010) with the addition of the Fermi-LAT measurement reported in Buehler et al. (2012). The pulsar spectrum is reproduced from Kuiper et al. (2001). Additionally shown are infrared measurements reported in Sollerman et al. (2000) and Tziamtzis et al. (2009), radio measurements referenced in Thompson et al. (1999) and gamma-ray measurements referenced in Fig. 8. Please note, that the low frequency radio data ($\lesssim 1$ GHz) comes from non-contemporaneous measurements, which are likely affected by time varying interstellar scintillation (Rickett & Lyne 1990). The luminosity shown on the right axis was calculated assuming a distance of 2 kpc.

and swings from $PA \approx 90°$ to $PA \approx 180°$ during P2.

2.2. The Crab nebula

The appearance of the nebula in the sky is approximately ellipsoidal with a major axis of ~ 7 arc minutes and a minor axis of ~ 4.6 arc minutes. This corresponds to a projected length of ~ 4.1 pc and ~ 2.7 pc, respectively. As one observes the nebula at higher frequencies, a toroidal structure becomes increasingly apparent. Images of the inner region in X-rays and optical are shown in Fig. 4. A torus surrounding the pulsar and a jet emerging perpendicular to it are apparent. It is striking that there is no bright emission in the region within ~ 10 arc seconds of the pulsar (Hester et al. 1995, Hester et al. 2002, Mori et al. 2004, Temim et al. 2006). The pulsar wind is apparently radiationless (or "cold"), until interaction with the ambient medium happens. The first interaction is commonly thought to occur at the "inner ring" observed in the X-ray image (Weisskopf et al. 2000).

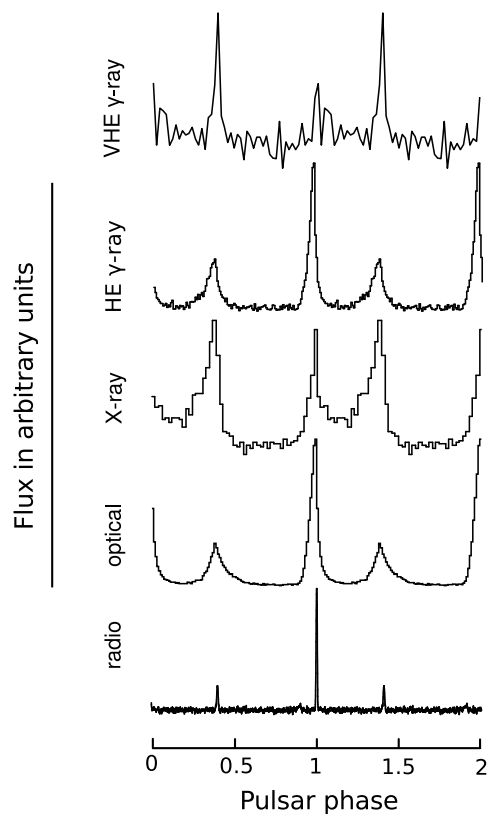As can be seen in Fig. 4, the inner nebula is a highly dynamical place. Thin arcs of

Figure 3. Flux as a function of phase for radio (1.4 GHz), optical ($1.5 - 3.5$ eV), X-ray ($100 - 200$ keV), HE gamma-ray ($100 - 300$ MeV) and VHE ($50 - 400$ GeV) gamma-ray energies. The data is reproduced from Du et al. (2012), with addition of the optical data from Oosterbroek et al. (2008) and VHE gamma-ray data from Aleksic et al. (2012).
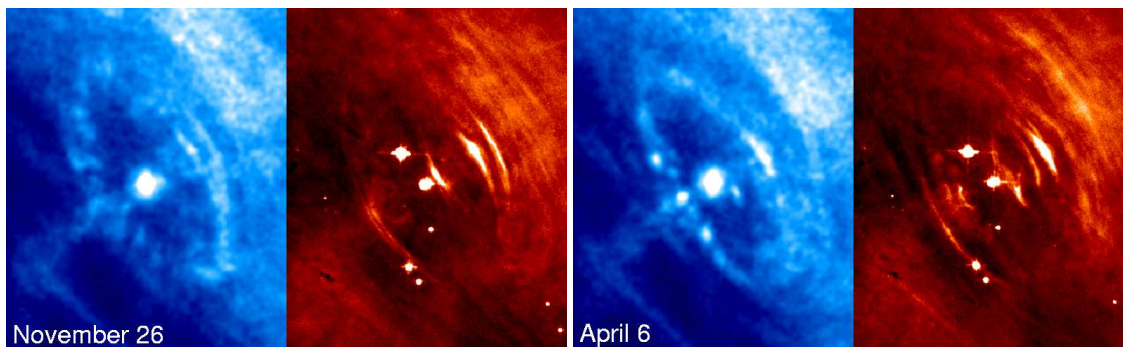

Figure 4. The inner region of the Crab nebula is shown for the 26th of November 2000 (left panels) and the 6th of April 2001 (right panels). The images were taken during simultaneous observations of the Chandra X-ray Observatory and the Hubble Space Telescope (Hester et al. 2002). The X-ray image is shown in blue colors, the optical image in red colors. The angular size of the image on the sky is 0.7 arc minutes in the horizontal direction and 0.6 arc minutes in the vertical direction (Hester 2013). Credits: X-ray: NASA/CXC/ASU/J. Hester et al.; Optical: NASA/HST/ASU/J. Hester et al..

increased emission, so called "wisps", are observed to move outwards from the inner ring into the body of the nebula (Scargle 1969). Wisps can be seen in radio, optical and X-rays, however their positions do not always coincide between frequencies. Typically, their inferred velocity is between 0.03 c and 0.5 c (Hester et al. 2002, Schweizer et al. 2013), with indications for radio wisps to be slightly slower (Bietenholz et al. 2001, Bietenholz et al. 2004). Additionally, several other structures on scales of a few arc seconds are seen close to the inner ring and along the jet. Most prominently the "Sprite" is seen as a fuzzy region at the base of the jet in the optical images, and the "inner knot"§ is detected only ~ 0.6 arc second south east of the pulsar (the inner knot is too close to the pulsar to be visible in Fig. 4, see e.g. Tziamtzis et al. (2009) or Moran et al. (2013)). Sprite, wisps and the inner knot are known to be variable down to time scales of a few hours (Hester et al. 2002, Melatos et al. 2005).

Spectrally, the nebula shows a trend to softer spectra with increasing distance from the pulsar. This is interpreted as the radiative cooling of the highest energy electrons as they are convected and diffuse away from the inner nebula. Interestingly however, the spectrum in the inner region of the nebula is rather uniform. The torus, the jet and the small scale structures mentioned in the previous paragraph show no strong spectral variations among them from infrared to X-ray energies (Veron-Cetty & Woltjer 1993, Willingale et al. 2001, Temim et al. 2006, Mori et al. 2004, Tziamtzis et al. 2009). At radio frequencies the picture is more complex. As radio emission originates from a larger volume in the nebula, it is generally more difficult to disentangle line of sight effects. However, also at radio frequencies the spectrum is harder in the inner nebula (Green et al. 2004, Arendt et al. 2011).

The emission from the nebula is found to be linearly polarized from radio to hard X-rays (Wilson 1974, Weisskopf et al. 1978, Bietenholz et al. 1991, Hester 2008, Dean et al. 2008, Forot et al. 2008, Aumont et al. 2010). Generally, the polarization angle $PA \approx 125°$ is aligned with the symmetry axis of the nebula, indicating that the magnetic fields are predominantly azimuthal. A detailed study was recently performed in optical by Moran et al. (2013). They find that the polarization of the wisps, the inner knot and the torus are all within a few degrees of the aforementioned PA and have a high degree of polarization $PD \sim 50\%$. While these structures are found to be variable in flux, their PA and PD show no significant variations.

The broad band SED of the nebula is shown in Fig. 2. One can see that the energy output of the nebula is a factor $\gtrsim 10$ larger than the one for the pulsar (in addition, the isotropic pulsar flux is likely even lower due to the beaming of its emission). In the nebula, the peak of the emission is located in the UV. The emission from radio to X-rays is known to be due to synchrotron emission thanks to polarization measurements. At high energies ($\gtrsim 400$ MeV), a second emission component emerges due to inverse Compton emission of the same electrons. This component is energetically subordinate with respect to the synchrotron emission by a factor $\gtrsim 100$.

§ There is some confusion with the nomenclature used in the literature. The "inner knot" is sometimes also referred to as "knot 1", and the "Sprite" sometimes referred to as "Anvil".
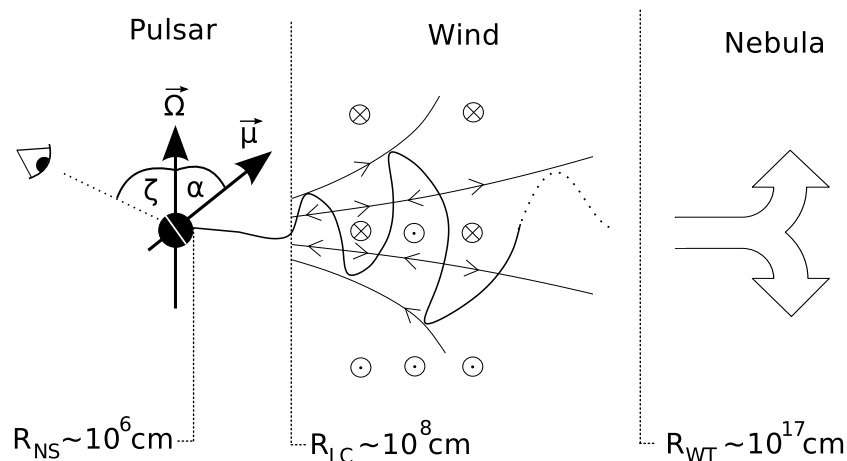
Figure 5. Sketch of the components of a pulsar wind nebula discussed in the text. The equatorial current sheet (thick straight line) and the magnetic fields (thin dashed line and circles) are shown in the wind region (see text). The geometry of the system is illustrated, with ζ being the angle of the observer with respect to the rotation vector of the pulsar Ω and α being the inclination of the magnetic moment μ of the pulsar with respect to Ω. For the Crab $\zeta \approx 60°$ was estimated assuming that Ω aligns with the symmetry axis of the nebula (Ng & Romani 2004). The angle α is unknown and typically inferred to be $\approx 45°$ from modeling of the pulsed emission (Harding et al. 2008, Du et al. 2012).

3. Theory of pulsar wind nebulae

To date ~ 100 pulsar wind nebulae have been detected, mostly at X-ray and TeV energies (Kargaltsev et al. 2013). The pulsar wind evolves inside of the supernova remnant of its progenitor star. Its time evolution is therefore complex, and depends on the properties of the progenitor and the environment in which it exploded. A review on pulsar wind nebulae evolution can be found in Gaensler & Slane (2006). In the following, we will focus on only on young systems (~ 1000 years), which have not yet been significantly disrupted by the reverse shock of their supernova remnant, or the proper motion of their pulsar. The Crab is the best studied of such systems.

In the common models of young pulsar wind nebula electrons and positrons are created in the magnetic fields of the pulsar and transported into the nebula. The electron density through most of the system is thereby expected to be large enough that magnetohydrodynamical conditions apply in good approximation. The pulsar wind is expected to carry most of the rotational energy lost by the pulsar into the nebula (Rees & Gunn 1974). The wind is flowing radiationless until its momentum flux is balanced by the ambient nebula pressure at a termination surface. At this surface, particles are randomized and begin to loose energy, predominantly through synchrotron radiation. Following these ideas the Crab can be subdivided in three regions shown in Fig. 5: (i) The pulsar and its magnetosphere which extends out to the light cylinder radius $R_{\rm LC} = \frac{cP}{2\pi} \approx 1.4 \times 10^8$ cm (ii) The cold pulsar wind which is though to extend out to the inner ring. In the plane perpendicular to the symmetry axis of the nebula the latter
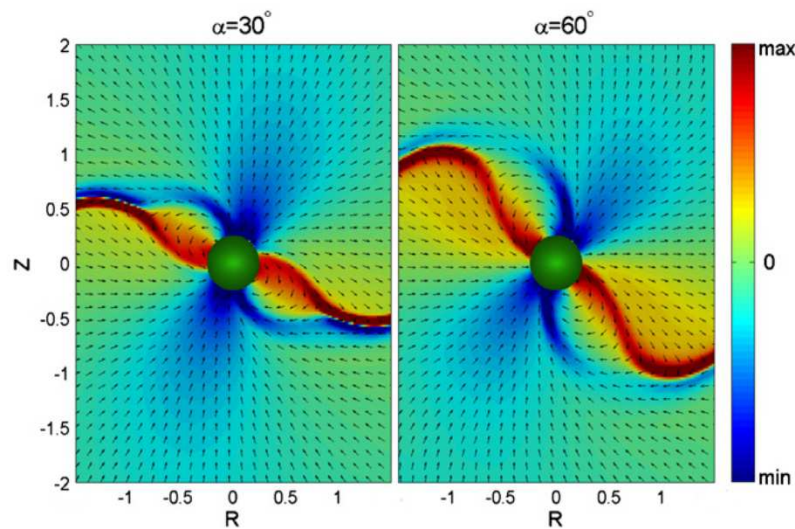
Figure 6. Force free simulation of a pulsar magnetosphere reproduced from Bai & Spitkovsky (2010a). Colors show of the charge density multiplied by the distance squared in the plane of the angular momentum Ω and magnetic moment μ of the pulsar. Results are shown for an inclination angle $\alpha = 30°$ and $60°$ between these two vectors. Arrows indicate the direction of the projected magnetic field. R and Z are in units of the light cylinder radius.

is located at $R_{\mathrm{WT}} \approx 3 \times 10^{17}$ cm (iii) The synchrotron nebula, which extends from the inner ring into the outer nebula. We will discuss each of these regions in the following.

3.1. The pulsar magnetosphere

A pulsar can be seen in first order as a rotating, perfectly conducting sphere, with a dipole magnetic field. The magnetic moment is generally not aligned with the rotational axis (the so called "oblique rotator"). Compression of the magnetic field of the progenitor star onto a neutron star of ~ 12 km diameter results in magnetic fields of the order of $B \approx 3.8 \times 10^{12}(\frac{P}{P_{\mathrm{Crab}}})^{1/2}(\frac{\dot{P}}{\dot{P}_{\mathrm{Crab}}})^{1/2}$ G at the equatorial surface of the neutron star. The rotation of this field induces an electric potential of the order of $\Delta\Phi \approx 4 \times 10^{16}(\frac{\dot{P}}{\dot{P}_{\mathrm{Crab}}})^{1/2}(\frac{P}{P_{\mathrm{Crab}}})^{-3/2}$ V between the poles and the equator of the star. After obtaining vacuum solutions of the oblique rotator (Deutsch 1955), it was realized that such strong potentials would remove particles from the neutron star surface and fill the magnetosphere with plasma. The magnetosphere becomes charge separated to compensate the electric potential (Goldreich & Julian 1969). This makes the calculation of the magnetosphere properties, as magnetic field structure and electric densities and currents, intrinsically non linear, and dependent on the microphysics of the neutron star surface and the magnetospheric plasma. We therefore still do not have a fully self-consistent description of the magnetosphere of pulsars.

Over the past decade however, there have been significant progress in our understanding of the magnetosphere using the force free electrodynamics (FFE) approximation. The FFE approximation can be derived from magnetohydrodynamics

(MHD) in the limit of inertia-free plasma, where the transport of energy and momentum is purely electromagnetical (Komissarov 2002, Blandford 2002). As in MHD, plasma is abundant and electric fields E parallel to the magnetic fields B are shortened out ($\vec{E} \cdot \vec{B} = 0$). There is no particle acceleration or resistivity. This approach is supported by the fact that modeling of pulsar wind nebulae suggest that electrons are injected at high rates from the magnetosphere into the nebula $\dot{N}_{+-} > 10^5 \times \dot{N}_{\mathrm{GJ}}$, where $\dot{N}_{\mathrm{GJ}} = 7.6 \times 10^{33} (\frac{P}{P_{\mathrm{Crab}}})^{-1/2} (\frac{\dot{P}}{\dot{P}_{\mathrm{Crab}}})^{1/2}$ s^{-1} is the "Goldreich-Julian" current (Bucciantini et al. 2011). Charge densities in the magnetosphere are therefore expected to significantly higher than the densities needed to compensate the electric potential due to pair creation within the magnetosphere (see Arons (2012) and references therein). Further supporting the FFE approximation is that only $\lesssim 10\%$ of the spin-down energy of pulsars is typically radiated in the form of pulsed emission, suggesting a low resistivity within the magnetosphere. Several simulations of magnetospheres in the FFE approximation have been made over the last years (Spitkovsky 2006, Kalapotharakos & Contopoulos 2009, Bai & Spitkovsky 2010a). The charge density and magnetic field structure in the plane of the angular moementum and magnetic moment vectors are shown in Fig. 6. The charge separation of the magnetosphere is apparent. A current sheet emerges in the equatorial plane, at the boundary between closed and open field lines‖ and crosses the light cylinder.

The FFE approximation cannot be exact, as there must be some resistivity in the magnetosphere. The latter depends on the properties of the co-rotating plasma, and has not been derived from first principles to date. However, ad-hoc introduction of resistivity into FFE and MHD simulations have been performed over the last years (Li et al. 2012, Kalapotharakos et al. 2012b, Kalapotharakos et al. 2012c, Tchekhovskoy et al. 2013). The basic magnetosphere properties, as e.g. the presence of the equatorial current sheet, are in agreement with the FFE approach. It was shown by Li et al. (2012) that the total spin-down luminosity and the potential drop over the open field lines transitions smoothly between the FFE approximation and the vacuum solution with increasing resistivity. The real magnetosphere of pulsars is therefore likely somewhere in between these two descriptions.

Neither MHD nor FFE simulations address the microphysics of the acceleration of particles within the magnetosphere. As currents flow out of the light cylinder on the open field lines, charge starved regions can emerge behind them (so called "gaps"). An electric potential drop can build up in these regions until it is discharged by electron pair cascades and particles are accelerated. A polar gap is thought to emerge up to a distance of $\lesssim 10^6$ cm above the magnetic poles (Sturrock 1971, Ruderman & Sutherland 1975, Holloway 1975, Daugherty & Harding 1982, Baring 2004). Gaps location have also been proposed out in the magnetosphere, along the last open field lines (slot gap (Arons & Scharlemann 1979, Muslimov & Harding 2004); annular gap (Qiao et al. 2004, Du et al. 2012)), reaching out to the light cylinder (outer gap

---

‖ Field lines which return to the pulsar within the light cylinder are usually referred to as "closed", others as "open".

(Cheng et al. 1976, Cheng et al. 1986, Romani & Yadigaroglu 1995, Cheng 2004)). Alternatively, particles might also be accelerated in reconnecting magnetic fields at the equatorial current sheet (Li et al. 2012, Tchekhovskoy et al. 2013). In either case, the particles loose their energy after leaving the acceleration region due to interaction with the magnetic and photon fields of the magnetosphere, and secondary particle cascades might be induced. As the direction of the particles is bound closely to the magnetic field lines, co-rotating cones of light are emitted around both magnetic poles. As one or both of them pass our line of sight, the observed electromagnetic pulsations are produced.

3.2. The cold pulsar wind

It was shown at the early days of pulsar studies, that the magnetic field lines become asymptotically radial beyond the light cylinder in the FFE approximation (Ingraham 1973, Michel 1974). This justified studying the fields and flows outside of the light cylinder in the "split-monopole" approximation, where the field lines from the pulsar are thought to be a monopole which inverses its field direction at the equator. An analytic solution to the obliquely rotating split-monopole was found by Bogovalov (1999). Generally, plasma that flows outside of the magnetosphere on the open field lines begins to trail the pulsar rotation, creating a helical pattern. A current sheet emerges which undulates within an angle α around the equatorial plane (the so called "striped wind"). The magnetic field lines become predominantly toroidal, and reverse their direction at the current sheet (see Fig. 5). Qualitative agreement with the split-monopole solutions has recently been found in FFE and MHD simulations out to a distance of $\lesssim 10 R_{\rm LC}$ (Kalapotharakos et al. 2012, Tchekhovskoy et al. 2013).

The Poynting flux per solid angle of the split monopole solution scales as $P \propto sin^2\theta$, where θ is the angle with respect to the rotation axis of the pulsar. As most of the energy is emitted around the equatorial plane, the striped wind plays an important role in the dynamics of the nebula. The wind is thought to be magnetically dominated at its launch, with $\sigma >> 1$, where σ is the ratio of the magnetic to the kinetic energy of the flow. However, as we will discuss in the next section a low-sigma flow of $\sigma \sim 0.003$ was inferred at the termination of the wind from 1D MHD modeling of the synchrotron nebula. The emerging question how magnetic energy is transferred to particle energy in the flow is referred to as the "σ-problem". In principle, at low latitudes the alternating magnetic fields of the striped wind make it susceptible to magnetic reconnection due to instabilities in the current flow (Coroniti 1990). However, it was realized that due to the relativistic motion of the wind, the time scales of these processes are likely too long (Lyubarsky & Kirk 2001, Kirk & Skjaraasen 2003). Recently, a new paradigm is emerging were magnetic energy is thought to be dissipated predominantly after the wind termination, as we will discuss in the next section.
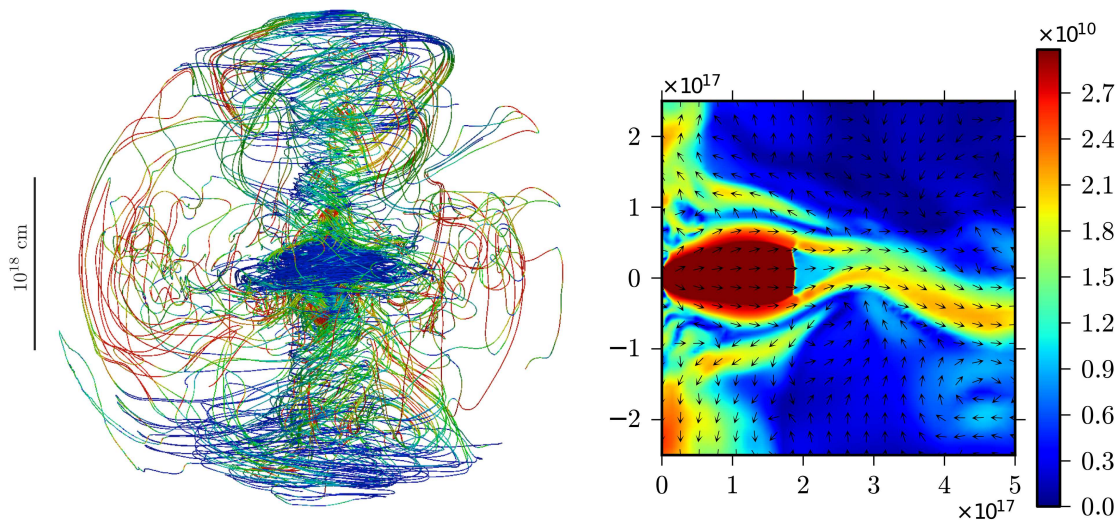
Figure 7. **Left:** sample magnetic field lines of a three dimensional MHD model of the Crab nebula with $\sigma = 3$, reproduced from Porth et al. (2013a). Colors indicate the dominating field component, blue for toroidal and red for poloidal. **Right:** velocity magnitude and direction of the plasma for the same simulation. Reproduced by permission of Oxford University Press.

3.3. The synchrotron nebula

As the cold pulsar wind can not be observed before it termination, its properties can only be inferred indirectly by observing the synchrotron nebula. Spherical symmetric MHD solution downstream of the termination surface were derived by Kennel & Coroniti (1984), predicting the magnetic field distribution in the nebula. The key parameter of this model is the magnetization of the wind just before its termination. In particular the distance of the termination surface from the pulsar in the Crab could only be reproduced if the magnetization at this point is low $\sigma \sim 0.003$. The magnetic field strength is then expected to increase behind the shock and have values between 100-300 μG in the synchrotron nebula (de Jager & Harding 1992, Atoyan & Aharonian 1996, Hillas et al. 1998, Meyer et al. 2010, Martin et al. 2012, Torres et al. 2013). This field is lower than the one expected in the case of equipartition between particle energy and magnetic fields, indicating that $\sim 1/30$ of the internal energy in the nebula is in magnetic form (Hillas et al. 1998). Similar magnetic field values are inferred by interpreting the hardening of the integrated spectrum of the nebula between the radio and the optical band due to electron cooling (Marsden et al. 1984).

It is typically assume that particles are re-accelerated at the wind termination surface. However, it is unlikely that diffusive shock acceleration of particles takes place, as the emerging shock is expected to be relativistic and oblique (Sironi & Spitkovsky 2011b). Instead, the turbulence downstream of the shock might trigger magnetic reconnection, which can lead to non-thermal particle acceleration (Lyubarsky 2003). Particle in cell (PIC) simulations show that, independent of the wind magnetization, the

energy of the alternating field components of the striped wind is dissipated into kinetic energy downstream of the wind termination (Sironi & Spitkovsky 2011a). Assuming that electrons are accelerated into a power-law spectrum at the termination surface one dimensional MHD models reproduces the spectral energy distribution of the nebula qualitatively, with the exception of the radio band (Atoyan & Aharonian 1996, Volpi et al. 2008). As the life time of radio emitting electrons is much longer than the age of the nebula, these particles might have been injected in the past. Radio emission might therefore come from a separate electron population, which could have been injected during the high spin-down phase of the pulsar following the super novae explosion (Atoyan & Aharonian 1996). Alternatively, radio emitting electrons could be continuously accelerated throughout the nebula due to magnetic reconnection in MHD turbulence (Nodes et al. 2004). Magnetic reconnection downstream of the wind termination can also reproduce the spectrum of radio emitting electrons, if electrons are injected at a rate of $\dot{N}_{+-} \sim 10^8 \times \dot{N}_{\mathrm{GJ}}$ into the pulsar wind and the magnetization is high with $\sigma > 30$ (Sironi & Spitkovsky 2011a). The implications of high electron multiplicities therefore deserve further study.

While the one dimensional models of the Crab laid out our general picture, it was clear form the beginning that the asymmetry of the nebula needs to be taken into account for a more quantitative description of the nebula. The dynamics of the flow at and beyond the wind termination have therefore been studied with multidimensional MHD simulations over the past decade (Komissarov & Lyubarsky 2004, Bucciantini et al. 2006, Porth et al. 2013a). The properties of the pulsar wind at its termination and the particle energy spectrum after the wind termination are free parameters of these simulations. Tracing the maximum particle energy in the flow makes it possible to compute synchrotron, inverse Compton and polarization maps of the nebula, which can be compared to observations (Del Zanna et al. 2006, Volpi et al. 2008, Volpi et al. 2009). Axially symmetric models with an appropriately chosen azimuthal dependence of the wind qualitatively reproduce the Crab morphology: a torus emerges, and the flow is bend backwards due to the "hoop-stress" in the downstream, creating a jet (see Fig. 7). They explain the emergence of wisps and their dynamics. Their increased brightness is thought to be predominately due to Doppler beaming towards our line of sight (Camus et al. 2009). The simulations predicted variability of a few percent per year in the overall X-ray emission of the nebula (Volpi et al. 2008), which has recently been discovered (Wilson-Hodge et al. 2011, Kouzu et al. 2013). This is remarkable in high-energy astrophysics, where predictions and measurements are seldom done on this level of accuracy.

As the early 1D MHD solution, the 2D simulations show that a low-sigma wind with $\sigma \sim 0.02$ matches the observed morphology, and the location the shock at the observed R_{WT}. Recently, the first 3D simulations were performed (Mizuno et al. 2011, Porth et al. 2013a, Porth et al. 2013b). Interestingly, these simulations show that the morphology of the Crab can also be obtained at high magnetization ($\sigma > 1$). As was pointed out by Begelman (1998), 1D and 2D MHD solutions prevent the growth

of turbulence due to current instabilities. Due to this turbulence, magnetic fields are randomized and remain predominantly axial only close to the wind termination (see Fig. 7), and pressure and magnetic field gradients in the nebula are reduced when compared to 1D or 2D models. The increased turbulence induces magnetic dissipation in the downstream, alleviating the σ-problem (Lyutikov 2010). While it might be too early for a final verdict, it appears that the origin of the latter lay in the simplifications made in 1D and 2D models.

The success of the MHD simulations in modeling many of the nebula's properties shows that the general picture we have outlined is likely a good approximation of reality. However, several observational findings can not be explained or have not been studied yet. A quantitative comparison of the morphology obtained in the simulations to the observed one has not been performed to date. In particular, the inner ring does not seem to be found consistently in the simulations. At odds with the expectation from Doppler boosting, the Chandra observations show that the inner ring has similar brightness at the front and the receding side. We also do not have an explanation why the ring appears to be composed of a series of knots, which are highly variable in time (Weisskopf et al. 2000, Porth et al. 2013b). The observation that the wisps at different wavebands are generally not aligned has not been studied in the simulations. If Doppler beaming is predominantly responsible for their enhanced brightness, one would naively expect radio, optical and X-ray wisps to be co-spatial. In addition, 2D MHD simulations with low magnetization overestimate the observed inverse Compton emission (Volpi et al. 2008). It will be interesting to see if this discrepancy is reduced in 3D models of high-magnetization.

4. Pulsed very high-energy gamma-ray emission

After having discussed the observational properties of the Crab and our theoretical understanding of pulsar wind nebulae, we will turn to the recent discoveries and their implications in the following. We begin with the detection of pulsed emission in VHE gamma rays. The emission of pulsars is typically expected to fall close to exponentially $\nu F_\nu \propto exp\left(\frac{E}{\epsilon_{\text{cut}}}\right)^b$ above a cutoff energy ϵ_{cut}. This cutoff is thought to be inherent to the emission mechanism, as we will discuss later. Indeed, all spectra of the ~ 150 pulsars detected to date at HE-gamma-rays are compatible with this expectation (Abdo et al. 2013). Surprisingly, a significantly slower spectral decay is observed for the Crab pulsar.

4.1. Observational results

The high-energy end of the SED of the Crab pulsar is shown in Fig. 8. The best fit parametrizations of the Fermi-LAT measurement by a power-law function with an exponential cutoff ($b = 1$) and a sub-exponential cutoff ($b < 1$) are also displayed. The latter parametrization is preferred statistically at a $\gtrsim 3\sigma$ confidence level, indicating
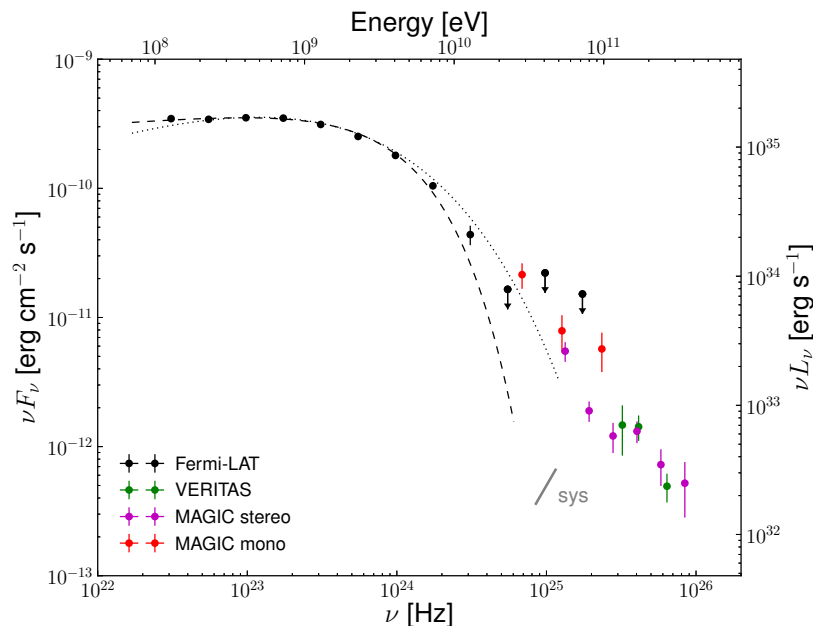
Figure 8. Phase averaged spectral energy distribution of the Crab pulsar in gamma-rays. The spectra are reproduced from Abdo et al. (2013), Aliu et al. (2011) , Aleksic et al. (2011) and Aleksic et al. (2012). The effect of systematic shifts of ±15% on the normalization of the energy scale is shown by the gray line. These are the typical systematic errors of VHE gamma-ray instruments. Best fit parametrizations of the Fermi-LAT data of a power-law function with an exponential (dashed) and sub-exponential (dotted) cutoff are shown (see text).

a slower than exponential fall of the spectrum. This is not unusual for LAT detected pulsars (Abdo et al. 2013). However, unexpectedly VHE gamma-ray measurements showed an enhanced emission above an extrapolation of both of these parametrizations (Aliu et al. 2008, Aliu et al. 2011, Aleksic et al. 2011, Aleksic et al. 2012) ¶. Considering systematic errors, the Fermi-LAT and VHE-gamma-ray data can be described by one power-law function above $E \approx 4$ GeV (Aliu et al. 2011). No indication of a spectral cutoff has been found up to photon energies of ~ 400 GeV.

The phase distribution of the VHE gamma-ray events is shown in Fig. 3. The peaks of the gamma-ray pulses coincide with the radio ones. Compared to the HE-gamma-ray pulsations, the VHE ones are narrower. This narrowing of the pulse width with increasing energy can also be seen in the HE and VHE data independently (Abdo et al. 2010, Aleksic et al. 2012). Interestingly, a hardening of the spectrum of $P2$ with respect to $P1$ is observed in similar form in two components of the SED: the relative flux of $P2$ increases with respect to $P1$ from radio to hard X-rays, and from HE gamma-rays to the VHE gamma-rays.

¶ Statistically marginal experimental discrepancies can be seen between different measurements in Fig. 8. In particular, the MAGIC mono data have larger fluxes compared to the other measurements. However, within systematic errors these differences are not significant.

4.2. The origin of the gamma-ray pulsations?

While radio emission from pulsars is usually attributed to coherent emission close to the polar gap, at higher frequencies the emission has to come from outer parts of the atmosphere. In particular the gamma-ray emission is expected to come from distance of $0.1 - 1R_{\mathrm{LC}}$ (Romani & Yadigaroglu 1995, Qiao et al. 2004, Muslimov & Harding 2004). This is inferred from the phasograms and spectra of the population of gamma-ray detected pulsars (Abdo et al. 2013). For the Crab pulsar, this expectation is confirmed in a model-independent way by the detection of emission beyond 100 GeV. To avoid absorption of gamma rays due to pair production on the pulsars magnetic fields, the photons have to be emitted at a distance $\sim 10^7$ cm $\approx 0.1R_{\mathrm{LC}}$ from the neutron star, a factor $\gtrsim 10$ above the expected location of the polar gap (Eq. 1 in Baring (2004)).

The emission mechanism at the high-energy end of the SED of pulsars is expected to be dominated by curvature radiation of particles streaming along magnetic field lines. However, the high energy of the pulsations makes this unlikely for the Crab. Radiative losses due to curvature radiation would produce a cutoff in the spectrum above gamma-ray energies of $\epsilon_{\mathrm{cut}} = 150$ GeV $(E/B)^{3/4}\sqrt{R/R_{\mathrm{LC}}}$, where E is the accelerating electric field (Aliu et al. 2011). The latter is typically assumed to be $E \lesssim 0.1B$ in pulsar gaps. The absence of a cutoff in the spectrum up to energies > 100 GeV therefore implies $R > R_{\mathrm{LC}}$. As particles stream along magnetic field lines only within the light cylinder, curvature radiation is likely not responsible for the VHE pulsations.

It was proposed by Lyutikov et al. (2012) that the emission at the high-energy end of the SED is dominated by Inverse Compton scattering. Indeed, the pulsed emission can be explained by up-scattering of photons in particle cascades induced by outer gaps (Aleksic et al. 2011, Aleksic et al. 2012) or annular gaps (Du et al. 2012). Alternatively, Inverse Compton emission can also occur in the striped wind (Bogovalov & Aharonian 2000, Kirk et al. 2002). As proposed by Aharonian et al. (2012) and Petri (2012), the VHE emission may result from the up-scatter of pulsed X-ray photons. If this is the case, the VHE observations are the first direct observational signature of the cold pulsar wind. In order to fit the observed pulse profile and spectrum of the VHE emission, the wind needs to be abruptly accelerated at $20 - 50R_{\mathrm{LC}}$. However, while the gamma-ray emission can be explained in this picture, the observed narrowing of the VHE pulses with increasing energy would not be expected.

5. Gamma-ray flux variations from the nebula

Flux variability on short time scales from structures within the Crab has been known for almost 100 years (Lampland 1921). However, the flux integrated over the volume of the nebula is varying only slowly over time: evidence for $\sim 1\%$ per year variations have been found in radio, optical and X-ray wavelength (Vinyaikin 2007, Smith 2003, Wilson-Hodge et al. 2011). As this is small compared to the systematic errors of most high energy telescopes, the Crab was often used to cross-calibrate instruments, particularly

in the X-ray and TeV domains. Stronger variability was generally expected to be found at the high end of the synchrotron component (~ 100 MeV), as this emission is expected to be emitted by particles with ~ 1 PeV energies in a ~ 0.1 mG magnetic field. The cooling time scales of these particles is ~ 1 year, and indeed indications for variability of $\sim 25\%$ over two years were found in this frequency range (Much et al. 1995, de Jager et al. 1996). Nevertheless, it came as a huge surprise when the Fermi-LAT and AGILE satellites detected strong gamma-ray flares, with increases of the unpulsed flux by a factor ~ 30 above 100 MeV on time scales down to ~ 6 hours (Abdo et al. 2011, Tavani et al. 2011, Balbo et al. 2011, Ackermann et al. 2013). We will discuss the observational results on the HE gamma-ray variability of the nebula in the following and summarize the theoretical conclusions drawn so far afterwards.

5.1. Observational results

The gamma-ray flares are observed in the energy range between the synchrotron and inverse Compton component of the spectral energy distribution. The average photon flux of the synchrotron component is $F_{\rm ns,100} = (6.1 \pm 0.2) \times 10^{-7}$ cm^{-2} s^{-1} and the one of the inverse Compton component is $F_{\rm ns,100} = (1.1 \pm 0.1) \times 10^{-7}$ cm^{-2} s^{-1} above 100 MeV. For comparison, photon flux of the pulsar above this energy is $F_{\rm p,100} = (20.4 \pm 0.1) \times 10^{-7}$ cm^{-2} s^{-1}. The emission of the inverse Compton component of the nebula and the pulsar flux are found to be constant in time within measurement accuracies. However, in the synchrotron nebula is variable on all time scales which can be resolved. The power density spectrum as a function of frequency of the flux variations is compatible with a power-law $PDS \propto \nu^{-0.9}$ (Buehler et al. 2012). The flux can remain below the detection threshold of the Fermi-LAT for a month, with flux upper limits well below the average flux value (Abdo et al. 2010). On the other hand, the flux can rapidly increase within a few hours during flares. Whether or not the flares are distinct events or the high-energy end of a continuous spectrum in variability is unclear. Time scales down to ≈ 10 hours can be resolved in the PDS with no sign of a break in the spectrum. However, the flares are far outlayers in the flux distribution and the spectrum during the brightest flares clearly shows the emergence of a new spectral component in the SED.

As of September 2013, six flares have been reported (Buehler et al. 2012, Ojha et al. 2012, Striani et al. 2013, Mayer et al. 2013). Due to the statistical nature of the flux variations, the definition of a flare is somewhat arbitrary. In all flares reported to date the synchrotron component of the nebula had a peak flux $F_{\rm ns,100} > 35 \times 10^{-7}$ cm^{-2} s^{-1}. Equally, the definition of a flare duration is not straight forward; typically, the flux is increased with respect to the monthly average flux for ~ 1 week. The SED around the peak of the flares is shown in Fig. 9. One can see that the spectral behavior differs strongly between flares. During the flare in February 2009, e.g. the flux increased with no measurable spectral changes with respect to the average nebula flux, while during the flare in April 2011 a new spectrum component with a rising flux was observed.
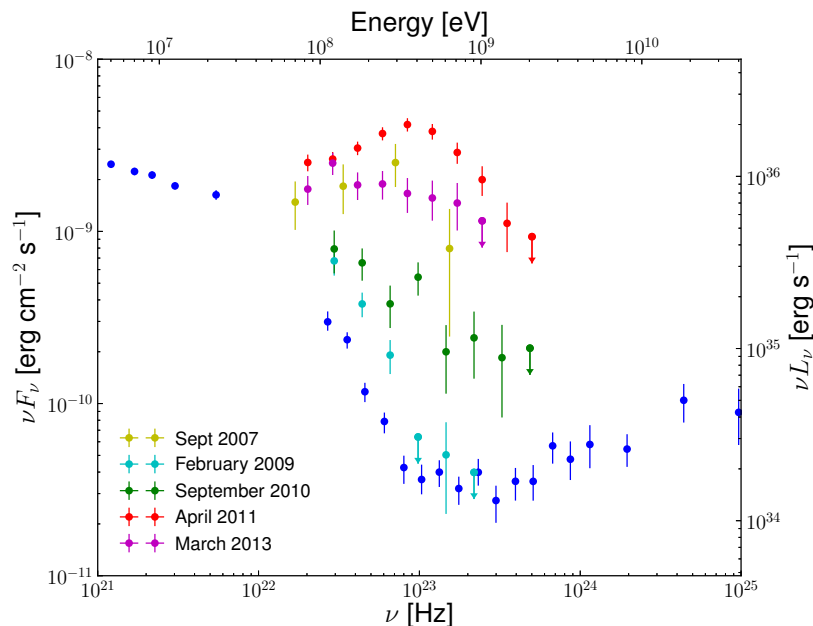
Figure 9. Spectral energy distribution at the maximum flux level for five of the six Crab nebula flares detected as of September 2013 (Abdo et al. 2011, Buehler et al. 2012, Striani et al. 2013, Mayer et al. 2013). No spectrum has been published for the low intensity flare of July 2012 (Ojha et al. 2012). The blue points show the average nebula flux values referenced in Fig. 2.

Generally, all spectra show significant emission up to ~ 1 GeV.

The flare of April 2011 gave us the most detailed look into the flare phenomenon to date (Striani et al. 2011, Buehler et al. 2012). The light curve of this flare is shown in Fig 10. Its high flux allowed flux measurements down to time scales of ~ 20 minutes. The flux doubled within $t_d \lesssim 8$ hours at the rising edges of the two main bursts during the flare. The spectral evolution is shown in Fig. 11. Interestingly, the apparently complex evolution can be parametrized in a simple way: the emerging spectral component is well characterized by a power-law spectrum with an exponential cutoff. The spectral index $\gamma = 1.27 \pm 0.12$ remains constant within errors during the flare, whereas the cutoff energy $E_{\rm C}$ and the total energy flux of the synchrotron component above 100 MeV vary as $L_{\rm ns,100} \propto E_{\rm C}^{3.42 \pm 0.86}$. At the maximum of the flare, the cutoff energy is $\epsilon_{\rm C,max} = 375 \pm 26$ MeV and the total isotropic luminosity in the synchrotron component is $L_{\rm max,100} \approx 4 \times 10^{36}$ erg s^{-1}, approximately 1% of the spin-down power of the pulsar.

The angular resolution of current HE instruments is > 18 arc minutes, not enough to determine the emission region of the flares within the nebula. From the beginning, it was clear that in order to pinpoint the emission region, correlated variability at radio, optical or X-rays is needed, making use of the < 1 arc second angular resolution achieved in these wavebands. However, to date, despite extensive efforts a detection of the flares outside of the HE gamma-ray band remains elusive. Strictly simultaneous observations were obtained during the September 2010, April 2011 and March 2013 flares (Vittorini
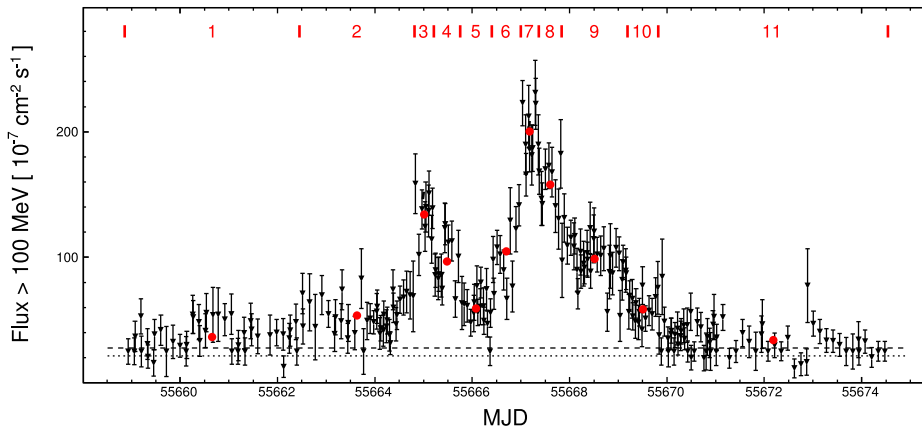
Figure 10. Integral flux above 100 MeV from the direction of the Crab as a function of time during the 2011 April flare, reproduced from Buehler et al. (2012). The points represent the sum of the nebula and pulsar fluxes. The dotted line indicates the sum of the 33-month average fluxes from the inverse-Compton nebula and the pulsar, which are stable over time. The dashed line shows the flux of the average synchrotron nebula summed to the latter. The red vertical lines indicate time intervals where the flux remains constant within statistical uncertainties. The time windows are enumerated at the top of the panel. The corresponding flux is shown by the red marker below each number. The SED for each of the time windows is shown in Figure 11.

et al. 2011, Morii et al. 2011, Lobanov et al. 2011, Weisskopf et al. 2013, Aliu et al. 2014). Particularly dense observations with the Chandra and Hubble Space Telescopes and the Keck and VLA Observatories were carried out during the April 2011 flare. No increased emission was detected from radio to X-rays for any structure of the nebula above the usual levels. This finding was very unexpected. The inferred flux upper limits show that the SED of the HE gamma-ray flare steeply drops with decreasing frequency, as was already suggested by the hard spectral index of the flaring component in HE gamma-rays during the flare.

No pulsations are found in the gamma-ray emission of the flares. The pulsar properties remain unchanged during the outbursts, no change in the spin-down period or flux were found in radio, X-rays or gamma-rays (Abdo et al. 2011, Morii et al. 2011, Buehler et al. 2012). The time scale of the recurrence of pulsar glitches is similar to the recurrence of the gamma-ray flares, however, there is no obvious correlation in time between these two events.

5.2. The origin of the gamma-ray flares?

To date, the Crab flares remain mysterious. We do not know what causes them and where they come from within the nebula. Several ideas have been proposed, but no definite answers can be given today. Any explanation will have to encompass *all* the presented observations, so far theoretical models have addressed different aspects of the problem. The rapid variability implies that, unless there is ultrarelativistic beaming,
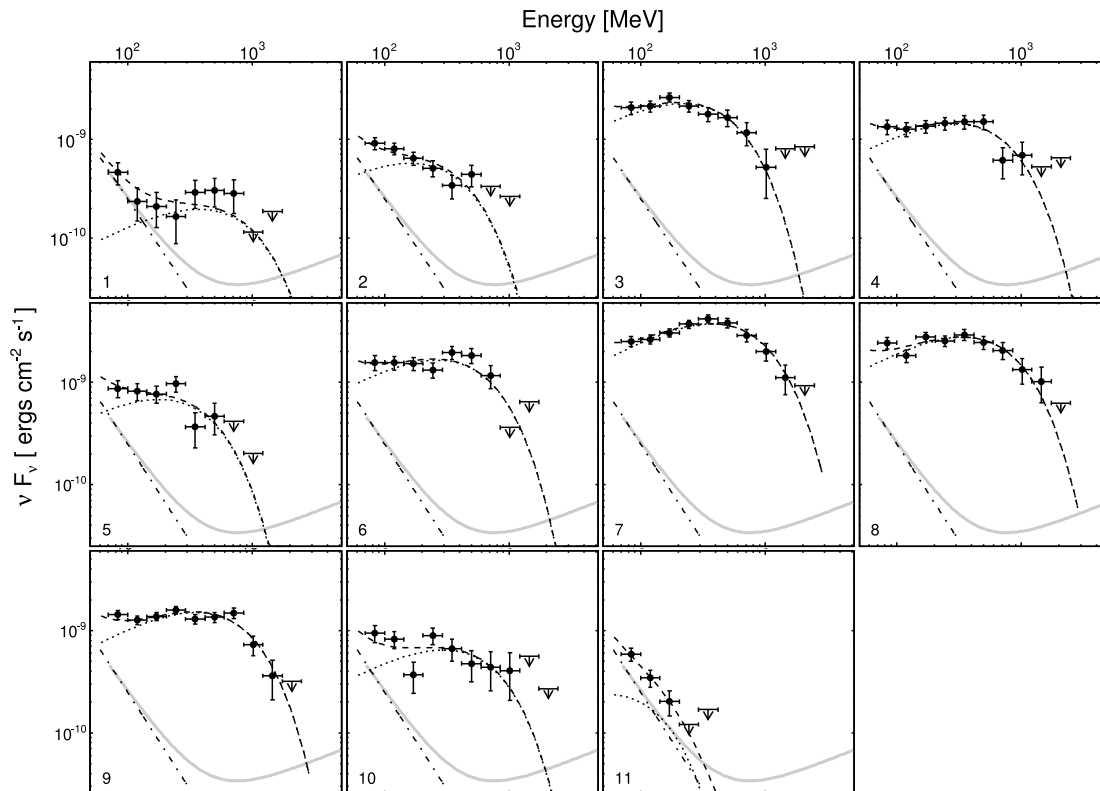
Figure 11. Spectral Energy Distribution evolution during the April 2011 Crab flare, reproduced from Buehler et al. (2012). The time windows are indicated in the bottom left corner of each panel and correspond to the ones indicated in Figure 10. The dotted line shows the SED of the flaring component, the dot-dashed line the constant background from the synchrotron nebula, and the dashed line is the sum of both components. The average Crab nebular spectrum in the first 33 months of *Fermi* observations is also shown in gray.

the flare emission comes from a small region within the nebula $R_{\rm f} \lesssim c \cdot t_d \approx 10^{-4}$ pc, small even when compared to nebula sub-structures as the Sprite, wisps or the inner knot with projected scales greater 10^{-2} pc.

A puzzling observation is that flare emission is detected up to photon energies of ≈ 1 GeV. Synchrotron emission appears to be the only radiation process which is efficient enough to account for the flare emission in the nebula environment (Abdo et al. 2011). However, particles accelerated in MHD flows can only emit synchrotron emission up to a maximum energy $\epsilon_{\rm max} = 160$ MeV (Guilbert et al. 1983, Uzdensky et al. 2011). Therefore, either MHD conditions are not valid in the flaring region, or the emission is relativistically boosted towards our line of sight [+]. Both scenarios are possibly interrelated: a breakdown of the MHD conditions occurs in magnetic reconnection

[+] Another alternative is that the flare emission is "jitter radiation", which could e.g. be emitted in the striped wind if the length scale of magnetic turbulence is much smaller than the distance between stripes (Teraki & Takahara 2013)

events and beaming of particles naturally occurs in the reconnection layer (Zweibel & Yamada 2009, Uzdensky et al. 2011, Cerutti et al. 2012, Sturrock & Aschwanden 2012).

That magnetic reconnection process is responsible for the particle acceleration is also indicated by the fact that the proposed alternatives have severe difficulties: diffusive shock acceleration generally does not produce electron spectra which are hard enough to explain the emission during the April 2011 flare and is expected to be inefficient at the termination of the pulsar wind (Ellison & Double 2004, Sironi & Spitkovsky 2011*b*, Sironi et al. 2013), and the proposed acceleration due to absorption of ion cyclotron waves is expected to act on longer time scales (Amato & Arons 2006). Magnetic reconnection was studied with PIC simulation in the context of the flares by Cerutti et al. (2013) and Baty et al. (2013). Cerutti et al. show that emission beyond ϵ_{max} is possible in such events. The variations in motion of the accelerated particle beams can explain the observed flux variations with a PDS compatible with the measured one. The spectrum of the April 2011 flare can be qualitatively reproduced, including its dynamical evolution and the observed correlation between cutoff energy and luminosity. The gamma-ray flares are therefore likely connected to explosive reconnection events triggered by current instabilities.

Regions with increased magnetic dissipation are the preferred emission sites, as e.g. downstream of the wind termination, near the inner ring (Bednarek & Idec 2011, Lyutikov et al. 2012, Bykov et al. 2012). In particular, at high latitudes the flow is expected to remain relativistic in the downstream and can be beamed into our line of sight. This produces increased emission from the so called "arch shock" of the wind termination, which was associated to the inner knot (Komissarov & Lyutikov 2011). Another possibility is that the flares originate from the base of the jet. As pointed out by Lyubarsky (2012), turbulence and increased magnetic dissipation are expected in this region, which might be associated to the Sprite. However, no observational signatures related to the flares have been found for any of these regions to date.

The location of the emission region might in principle be different between flares. A distribution of flares throughout the nebula has been proposed, where the beamed gamma-ray emission from different regions randomly crosses our line of sight (Yuan et al. 2011, Clausen-Brown & Lyutikov 2012). Such a process can produce PDS of flux variations compatible with the observed one, linking the flare phenomenon to the flux variations on longer time scales. The flares might therefore be responsible for a significant part of the magnetic dissipation in the nebula (Komissarov 2012).

6. Outlook

A review of the observations and theory of the Crab is bound to be outdated as it is written. New insights are gained continuously and building up on a long history of research. Nevertheless, key questions for our understanding remain unanswered. In particular, the structure of the magnetosphere, and related to it, the launch of the pulsar wind, remain to be understood in a quantitative way. The observed pulse

profiles are sensitive probes of the magnetic field structure and of the sites particle acceleration in the magnetosphere (Bai & Spitkovsky 2010*b*). Pulsar emission models can be compared to a wealth of observational data, including phase profiles, spectra and polarization measurements of the pulsar population. The latter is continuously growing, in particular through the ongoing observations of the Fermi-LAT. At the same time, emission models can take advantage of the increasingly more realistic simulations of pulsar magnetospheres.

Such a broad modeling approach is currently being pursued by several groups, and bears large potential to increase our understanding of pulsars (Bai & Spitkovsky 2010*a*, Romani & Watters 2010, Harding et al. 2011, Kalapotharakos et al. 2012). The VHE gamma-ray pulsations of the Crab are a new constraint which needs to be addressed within this context. Experimentally, it remains to be seen whether VHE emission is typical for pulsars or only found in the Crab (Collaboration 2013). Searches by current VHE instruments for pulsations from other pulsars are ongoing. The future Cherenkov Telescope Array (CTA) will allow to perform these searches at higher sensitivities (Acharya et al. 2013).

The understanding of the Crab synchrotron nebula has significantly increased with the help of MHD simulations in the last years. Quantitative comparisons of observations to these simulations can constrain the magnetization and angular dependence of the pulsar wind. First three dimensional simulations show that significant magnetic dissipation is expected to happen downstream of the wind termination (Porth et al. 2013*a*). The gamma-ray flares are an exciting discovery in this context, likely giving us a direct view into magnetic dissipation regions.

It is puzzling that flares have not been detected from any other pulsar wind nebula besides the Crab. The search of flares from other nebulae is ongoing in the HE-gamma-ray band (Ackermann et al. 2013). Giving the unusually large magnetization of the Crab nebula, flare might be found at lower frequencies in other systems. In this case, all-sky X-ray instruments as MAXI are best suited to search for flares from other nebulae (Matsuoka et al. 2009). The HE gamma-ray flares from the Crab have been recurring approximately once per year. Dense multi-waveband coverage in the radio, optical, X-ray and VHE gamma-ray bands was achieved during the last flare in March 2013 (Mayer et al. 2013). The analysis of these observations is still ongoing and might already reveal correlated signatures to the HE-gamma-ray variability. Monitoring programs are already put in place for future flares. The continuous multi-wavelength coverage will enable more sensitive correlation studies and hopefully pinpoint the emission site in the coming years. Also, the detection of an inverse Compton component of the flares at VHE gamma-rays might be possible with CTA in the future, if the emission region is ultra-relativistically beamed towards our line of sight (Lorentz factor $\gtrsim 30$, Kohri et al. (2012)).

In a broader context, several phenomena observed in the Crab are ubiquitous in the non-thermal Universe. A better understanding of the Crab, and pulsar wind nebulae in general, is therefore interweaved with our understanding of other sources as active

galaxies, microquasars, gamma-ray bursts or novae. The release of magnetic energy by a compact object, and the transfer of this energy into the acceleration of particles is common in these systems. Formation of jets is also ubiquitous in non-thermal sources. This process can be studied in detail in the synchrotron nebula of the Crab. As e.g., the study of the dynamics and formation of the wisps, the jet formation in the Crab allows us to study the behavior of relativistic magnetized plasma and the instabilities that govern its flow (Mignone et al. 2013). The remainders of the "guest star" observed almost one thousand years ago will continue to be our companion in these endeavors.

Acknowledgments

References

Abdo et al. 2011 *Science (New York, N.Y.)* **331**(6018), 739–42.
    URL: *http://adsabs.harvard.edu/abs/2011Sci...331..739A*
Abdo et al. 2010 *The Astrophysical Journal* **708**(2), 1254–1267.
    URL: *http://adsabs.harvard.edu/abs/2010ApJ...708.1254A*
Abdo et al. 2013 *The Astrophysical Journal Supplement Series* **208**(2), 17.
    URL: *http://adsabs.harvard.edu/abs/2013ApJS..208...17A*
Acharya et al. 2013 *Astroparticle Physics* **43**, 3–18.
    URL: *http://www.sciencedirect.com/science/article/pii/S0927650513000169*
Ackermann et al. 2013 *The Astrophysical Journal* **771**(1), 57.
    URL: *http://iopscience.iop.org/0004-637X/771/1/57/article/*
Aharonian et al. 2012 *Nature* **482**(7386), 507–9.
    URL: *http://adsabs.harvard.edu/abs/2012Natur.482..507A*
Aleksic et al. 2012 *Astronomy & Astrophysics* **540**, A69.
    URL: *http://www.aanda.org/10.1051/0004-6361/201118166*
Aleksic et al. 2011 *The Astrophysical Journal* **742**(1), 43.
    URL: *http://adsabs.harvard.edu/abs/2011ApJ...742...43A*
Aliu et al. 2008 *Science (New York, N.Y.)* **322**(5905), 1221–4.
    URL: *http://adsabs.harvard.edu/abs/2008Sci...322.1221A*
Aliu et al. 2012 *The Astrophysical Journal* **760**(2), 136.
    URL: *http://adsabs.harvard.edu/abs/2012ApJ...760..136A*
Aliu et al. 2014 *The Astrophysical Journal* **781**(1), L11.
    URL: *http://adsabs.harvard.edu/abs/2014ApJ...781L..11A*
Aliu et al. 2011 *Science (New York, N.Y.)* **334**(6052), 69–72.
    URL: *http://adsabs.harvard.edu/abs/2011Sci...334...69V*
Amato & Arons 2006 *The Astrophysical Journal* **653**(1), 325–338.
    URL: *http://adsabs.harvard.edu/abs/2006ApJ...653..325A*

Arendt et al. 2011 *The Astrophysical Journal* **734**(1), 54.
    URL: *http://adsabs.harvard.edu/abs/2011ApJ...734...54A*

Arons 2012 *Space Science Reviews* **173**(1-4), 341–367.
    URL: *http://adsabs.harvard.edu/abs/2012SSRv..173..341A*

Arons & Scharlemann 1979 *The Astrophysical Journal* **231**, 854.
    URL: *http://adsabs.harvard.edu/abs/1979ApJ...231..854A*

Atoyan & Aharonian 1996 *Monthly Notices of the Royal Astronomical Society* **278**(2), 525–541.
    URL: *http://adsabs.harvard.edu/abs/1996MNRAS.278..525A*

Aumont et al. 2010 *Astronomy and Astrophysics* **514**, A70.
    URL: *http://adsabs.harvard.edu/abs/2010A&A...514A..70A*

Baade & Zwicky 1934 *Physical Review* **46**(1), 76–77.
    URL: *http://adsabs.harvard.edu/abs/1934PhRv...46...76B*

Bai & Spitkovsky 2010*a* *The Astrophysical Journal* **715**(2), 1282–1301.
    URL: *http://iopscience.iop.org/0004-637X/715/2/1282/fulltext/*

Bai & Spitkovsky 2010*b* *The Astrophysical Journal* **715**(2), 1270–1281.
    URL: *http://iopscience.iop.org/0004-637X/715/2/1270/fulltext/*

Balbo et al. 2011 *Astronomy & Astrophysics* **527**, L4.
    URL: *http://adsabs.harvard.edu/abs/2011A&A...527L...4B*

Baring 2004 *Advances in Space Research* **33**(4), 552–560.
    URL: *http://adsabs.harvard.edu/abs/2004AdSpR..33..552B*

Baty et al. 2013 *Monthly Notices of the Royal Astronomical Society* **436**(1).
    URL: *http://adsabs.harvard.edu/abs/2013arXiv1308.0906B*

Bednarek & Idec 2011 *Monthly Notices of the Royal Astronomical Society* **414**(3), 2229–2234.
    URL: *http://adsabs.harvard.edu/abs/2011MNRAS.414.2229B*

Begelman 1998 *The Astrophysical Journal* **493**(1), 291–300.
    URL: *http://iopscience.iop.org/0004-637X/493/1/291/fulltext/*

Bietenholz et al. 2001 *The Astrophysical Journal* **560**(1), 254–260.
    URL: *http://iopscience.iop.org/0004-637X/560/1/254/fulltext/*

Bietenholz et al. 2004 *The Astrophysical Journal* **615**(2), 794–804.
    URL: *http://adsabs.harvard.edu/abs/2004ApJ...615..794B*

Bietenholz et al. 1991 *The Astrophysical Journal* **373**, L59.
    URL: *http://adsabs.harvard.edu/abs/1991ApJ...373L..59B*

Bilous et al. 2011 *The Astrophysical Journal* **728**(2), 110.
    URL: *http://adsabs.harvard.edu/abs/2011ApJ...728..110B*

Bilous et al. 2012 *The Astrophysical Journal* **749**(1), 24.
    URL: *http://adsabs.harvard.edu/abs/2012ApJ...749...24B*

Blandford 2002 *Lighthouses of the Universe: The Most Luminous Celestial Objects and Their Use for Cosmology* ESO ASTROPHYSICS SYMPOSIA
    URL: *http://adsabs.harvard.edu/abs/2002luml.conf..381B*

Bogovalov 1999 *Astronomy and Astrophysics* **349**, 1017.
    URL: *http://adsabs.harvard.edu/abs/1999A&A...349.1017B*

Bogovalov & Aharonian 2000 *Monthly Notices of the Royal Astronomical Society* **313**(3), 504–514.
    URL: *http://adsabs.harvard.edu/abs/2000MNRAS.313..504B*

Breen & McCarthy 1995 *Vistas in Astronomy* **39**(3), 363–379.
    URL: *http://dx.doi.org/10.1016/0083-6656(95)96619-S*

Bucciantini et al. 2011 *Monthly Notices of the Royal Astronomical Society* **410**(1), 381–398.
    URL: *http://adsabs.harvard.edu/abs/2011MNRAS.410..381B*

Bucciantini et al. 2006 *Monthly Notices of the Royal Astronomical Society* **368**(4), 1717–1734.
    URL: *http://adsabs.harvard.edu/abs/2006MNRAS.368.1717B*

Buehler et al. 2012 *The Astrophysical Journal* **749**(1), 26.
    URL: *http://iopscience.iop.org/0004-637X/749/1/26/*

Bykov et al. 2012 *Monthly Notices of the Royal Astronomical Society: Letters* **421**(1), L67–L71.
    URL: *http://adsabs.harvard.edu/abs/2012MNRAS.421L..67B*

Camus et al. 2009 *Monthly Notices of the Royal Astronomical Society* **400**(3), 1241–1246.
    URL: *http://adsabs.harvard.edu/abs/2009MNRAS.400.1241C*

Cerutti et al. 2012 *The Astrophysical Journal* **746**(2), 148.
    URL: *http://adsabs.harvard.edu/abs/2012ApJ...746..148C*

Cerutti et al. 2013 *eprint* **1302.6247**.
    URL: *http://adsabs.harvard.edu/abs/2013arXiv1302.6247C*

Cheng et al. 1976 *The Astrophysical Journal* **203**, 209.
    URL: *http://adsabs.harvard.edu/abs/1976ApJ...203..209C*

Cheng 2004 *Advances in Space Research* **33**(4), 561–570.
    URL: *http://adsabs.harvard.edu/abs/2004AdSpR..33..561C*

Cheng et al. 1986 *The Astrophysical Journal* **300**, 500.
    URL: *http://adsabs.harvard.edu/abs/1986ApJ...300..500C*

Clausen-Brown & Lyutikov 2012 *Monthly Notices of the Royal Astronomical Society* **426**(2), 1374.
    URL: *http://adsabs.harvard.edu/abs/2012arXiv1205.5094C*

Cocke et al. 1969 *Nature* **221**(5180), 525–527.
    URL: *http://adsabs.harvard.edu/abs/1969Natur.221..525C*

Collaboration 2013 *eprint* **1306.6772**.
    URL: *http://adsabs.harvard.edu/abs/2013arXiv1306.6772T*

Cordes et al. 2004 *The Astrophysical Journal* **612**(1), 375–388.
    URL: *http://adsabs.harvard.edu/abs/2004ApJ...612..375C*

Coroniti 1990 *The Astrophysical Journal* **349**, 538.
    URL: *http://adsabs.harvard.edu/abs/1990ApJ...349..538C*

Daugherty & Harding 1982 *The Astrophysical Journal* **252**, 337.
    URL: *http://adsabs.harvard.edu/abs/1982ApJ...252..337D*

de Jager & Harding 1992 *The Astrophysical Journal* **396**, 161.
    URL: *http://adsabs.harvard.edu/abs/1992ApJ...396..161D*

de Jager et al. 1996 *The Astrophysical Journal* **457**, 253.
    URL: *http://adsabs.harvard.edu/abs/1996ApJ...457..253D*

Dean et al. 2008 *Science (New York, N.Y.)* **321**(5893), 1183–5.
    URL: *http://adsabs.harvard.edu/abs/2008Sci...321.1183D*

Del Zanna et al. 2006 *Astronomy and Astrophysics* **453**(2), 621–633.
    URL: *http://dx.doi.org/10.1051/0004-6361:20064858*

Deutsch 1955 *Annales d'Astrophysique* **18**(1).
    URL: *http://adsabs.harvard.edu/abs/1955AnAp...18....1D*

Du et al. 2012 *The Astrophysical Journal* **748**(2), 84.
    URL: *http://adsabs.harvard.edu/abs/2012ApJ...748...84D*

Ellison & Double 2004 *Astroparticle Physics* **22**(3-4), 323–338.
    URL: *http://adsabs.harvard.edu/abs/2004APh....22..323E*

Espinoza et al. 2011 *The Astronomer's Telegram* **3777**.
    URL: *http://adsabs.harvard.edu/abs/2011ATel.3777....1E*

Forot et al. 2008 *The Astrophysical Journal* **688**(1), L29–L32.
    URL: *http://adsabs.harvard.edu/abs/2008ApJ...688L..29F*

Gaensler & Slane 2006 *Annual Review of Astronomy and Astrophysics* **44**(1), 17–47.
    URL: *http://adsabs.harvard.edu/abs/2006ARA&A..44...17G*

Gallant & Arons 1994 *The Astrophysical Journal* **435**, 230.
    URL: *http://adsabs.harvard.edu/abs/1994ApJ...435..230G*

Gold 1968 *Nature* **218**(5143), 731–732.
    URL: *http://adsabs.harvard.edu/abs/1968Natur.218..731G*

Goldreich & Julian 1969 *The Astrophysical Journal* **157**, 869.

URL: *http://adsabs.harvard.edu/abs/1969ApJ...157..869G*

Green et al. 2004 *Monthly Notices of the Royal Astronomical Society* **355**(4), 1315–1326.
    URL: *http://adsabs.harvard.edu/abs/2004MNRAS.355.1315G*

Guilbert et al. 1983 *Monthly Notices of the Royal Astronomical Society (ISSN 0035-8711)* **205**, 593–603.
    URL: *http://adsabs.harvard.edu/abs/1983MNRAS.205..593G*

Harding 2013 *Frontiers of Physics* **8**(6), 679.
    URL: *http://adsabs.harvard.edu/abs/2013arXiv1302.0869H*

Harding et al. 2011 *eprint* **1111.0828**.
    URL: *http://adsabs.harvard.edu/abs/2011arXiv1111.0828H*

Harding et al. 2008 *The Astrophysical Journal* **680**(2), 1378–1393.
    URL: *http://adsabs.harvard.edu/abs/2008ApJ...680.1378H*

Hester 2013 *webpage* .
    URL: *http://chandra.harvard.edu/photo/2002/0052/more.html*

Hester 2008 *Annual Review of Astronomy and Astrophysics* **46**(1), 127–155.
    URL: *http://adsabs.harvard.edu/abs/2008ARA&A..46..127H*

Hester et al. 2002 *The Astrophysical Journal* **577**(1), L49–L52.
    URL: *http://adsabs.harvard.edu/abs/2002ApJ...577L..49H*

Hester et al. 1995 *The Astrophysical Journal* **448**, 240.
    URL: *http://adsabs.harvard.edu/abs/1995ApJ...448..240H*

Hillas et al. 1998 *The Astrophysical Journal* **503**(2), 744–759.
    URL: *http://iopscience.iop.org/0004-637X/503/2/744/fulltext/*

Holloway 1975 *Monthly Notices of the Royal Astronomical Society* **171**, 619–635.
    URL: *http://adsabs.harvard.edu/abs/1975MNRAS.171..619H*

Hubble 1928 *Astronomical Society of the Pacific Leaflets* **1**(14), 55.
    URL: *http://adsabs.harvard.edu/abs/1928ASPL....1...55H*

Ingraham 1973 *The Astrophysical Journal* **186**, 625.
    URL: *http://adsabs.harvard.edu/abs/1973ApJ...186..625I*

Kalapotharakos & Contopoulos 2009 *Astronomy and Astrophysics* **496**(2), 495–502.
    URL: *http://adsabs.harvard.edu/abs/2009A&A...496..495K*

Kalapotharakos et al. 2012 *Monthly Notices of the Royal Astronomical Society* **420**(4), 2793–2798.
    URL: *http://mnras.oxfordjournals.org/content/420/4/2793*

Kalapotharakos et al. 2012b *The Astrophysical Journal* **754**(1), L1.
    URL: *http://adsabs.harvard.edu/abs/2012ApJ...754L...1K*

Kalapotharakos et al. 2012c *The Astrophysical Journal* **749**(1), 2.
    URL: *http://adsabs.harvard.edu/abs/2012ApJ...749....2K*

Kargaltsev et al. 2013 *eprint* **1305.2552**.
    URL: *http://adsabs.harvard.edu/abs/2013arXiv1305.2552K*

Kennel & Coroniti 1984 *The Astrophysical Journal* **283**, 694.
    URL: *http://adsabs.harvard.edu/abs/1984ApJ...283..694K*

Kirk & Lyubarsky 2009 *in* 'Neutron Stars and Pulsars' Vol. 357 Springer Berlin Heidelberg pp. 421–450.

Kirk & Skjaraasen 2003 *The Astrophysical Journal* **591**(1), 366–379.
    URL: *http://adsabs.harvard.edu/abs/2003ApJ...591..366K*

Kirk et al. 2002 *Astronomy and Astrophysics* **388**(2), L29–L32.
    URL: *http://adsabs.harvard.edu/abs/2002A&A...388L..29K*

Kohri et al. 2012 *Monthly Notices of the Royal Astronomical Society* **424**(3), 2249–2254.
    URL: *http://adsabs.harvard.edu/abs/2012MNRAS.424.2249K*

Komissarov 2002 *Monthly Notices of the Royal Astronomical Society* **336**(3), 759–766.
    URL: *http://adsabs.harvard.edu/abs/2002MNRAS.336..759K*

Komissarov 2012 *Monthly Notices of the Royal Astronomical Society* **428**(3), 2459–2466.
    URL: *http://adsabs.harvard.edu/abs/2013MNRAS.428.2459K*

Komissarov & Lyubarsky 2004 *Monthly Notices of the Royal Astronomical Society* **349**(3), 779–792.
    URL: *http://mnras.oxfordjournals.org/content/349/3/779*
Komissarov & Lyutikov 2011 *Monthly Notices of the Royal Astronomical Society* **414**(3), 2017–2028.
    URL: *http://adsabs.harvard.edu/abs/2011MNRAS.414.2017K*
Kouzu et al. 2013 *Publications of the Astronomical Society of Japan* **65**(4), 74.
    URL: *http://adsabs.harvard.edu/abs/2013arXiv1303.7109K*
Kuiper et al. 2001 *Astronomy and Astrophysics* **378**(3), 918–935.
    URL: *http://adsabs.harvard.edu/abs/2001A&A...378..918K*
Lampland 1921 *Publications of the Astronomical Society of the Pacific* **33**, 79.
    URL: *http://adsabs.harvard.edu/abs/1921PASP...33...79L*
Li et al. 2012 *The Astrophysical Journal* **746**(1), 60.
    URL: *http://iopscience.iop.org/0004-637X/746/1/60/fulltext/*
Lobanov et al. 2011 *Astronomy & Astrophysics* **533**, A10.
    URL: *http://adsabs.harvard.edu/abs/2011A&A...533A..10L*
Lundgren et al. 1995 *The Astrophysical Journal* **453**, 433.
    URL: *http://adsabs.harvard.edu/abs/1995ApJ...453..433L*
Lyne et al. 1993 *Monthly Notices of the Royal Astronomical Society* **265**.
    URL: *http://adsabs.harvard.edu/abs/1993MNRAS.265.1003L*
Lyubarsky 2003 *Monthly Notices of the Royal Astronomical Society* **345**(1), 153–160.
    URL: *http://adsabs.harvard.edu/abs/2003MNRAS.345..153L*
Lyubarsky 2012 *Monthly Notices of the Royal Astronomical Society* **427**(2), 1497–1502.
    URL: *http://mnras.oxfordjournals.org/content/427/2/1497*
Lyubarsky & Kirk 2001 *The Astrophysical Journal* **547**(1), 437–448.
    URL: *http://adsabs.harvard.edu/abs/2001ApJ...547..437L*
Lyutikov 2010 *Monthly Notices of the Royal Astronomical Society* **405**(3), 1809.
    URL: *http://adsabs.harvard.edu/abs/2010MNRAS.405.1809L*
Lyutikov et al. 2012 *Monthly Notices of the Royal Astronomical Society* **422**(4), 3118–3129.
    URL: *http://adsabs.harvard.edu/abs/2012MNRAS.422.3118L*
Manchester et al. 2005 *The Astronomical Journal* **129**(4), 1993–2006.
    URL: *http://adsabs.harvard.edu/abs/2005AJ....129.1993M*
Marsden et al. 1984 *The Astrophysical Journal* **278**, L29.
    URL: *http://adsabs.harvard.edu/abs/1984ApJ...278L..29M*
Martin et al. 2012 *Monthly Notices of the Royal Astronomical Society* **427**(1), 415–427.
    URL: *http://adsabs.harvard.edu/abs/2012MNRAS.427..415M*
Matsuoka et al. 2009 *Publications of the Astronomical Society of Japan* **61**(5), 999.
    URL: *http://adsabs.harvard.edu/abs/2009PASJ...61..999M*
Mayer et al. 2013 *The Astrophysical Journal* **775**(2), L37.
    URL: *http://iopscience.iop.org/2041-8205/775/2/L37/article/*
Melatos et al. 2005 *The Astrophysical Journal* **633**(2), 931–940.
    URL: *http://adsabs.harvard.edu/abs/2005ApJ...633..931M*
Meyer et al. 2010 *Astronomy & Astrophysics* **523**, A2.
    URL: *http://adsabs.harvard.edu/abs/2010A&A...523A...2M*
Michel 1974 *Astrophysical Journal* **187**, 585–588.
    URL: *http://adsabs.harvard.edu/abs/1974ApJ...187..585M*
Mignone et al. 2013 *Monthly Notices of the Royal Astronomical Society* **436**(2), 1102.
    URL: *http://adsabs.harvard.edu/abs/2013MNRAS.436.1102M*
Mizuno et al. 2011 *The Astrophysical Journal* **728**(2), 90.
    URL: *http://iopscience.iop.org/0004-637X/728/2/90/fulltext/*
Moffett et al. 1999 *The Astrophysical Journal* **522**(2), 1046.
    URL: *http://adsabs.harvard.edu/abs/1999ApJ...522.1046M*
Moran et al. 2013 *Monthly Notices of the Royal Astronomical Society* **433**(3), 2564–2575.

URL: *http://adsabs.harvard.edu/abs/2013MNRAS.433.2564M*
Mori et al. 2004 *The Astrophysical Journal* **609**(1), 186–193.
    URL: *http://iopscience.iop.org/0004-637X/609/1/186/fulltext/*
Morii et al. 2011 *Journal of Physics: Conference Series* **302**(1), 012062.
    URL: *http://adsabs.harvard.edu/abs/2011JPhCS.302a2062M*
Much et al. 1995 *Astronomy and Astrophysics* **299**, 435.
    URL: *http://adsabs.harvard.edu/abs/1995A&A...299..435M*
Muslimov & Harding 2004 *The Astrophysical Journal* **606**(2), 1143–1153.
    URL: *http://adsabs.harvard.edu/abs/2004ApJ...606.1143M*
Ng & Romani 2004 *The Astrophysical Journal* **601**(1), 479–484.
    URL: *http://adsabs.harvard.edu/abs/2004ApJ...601..479N*
Nodes et al. 2004 *Astronomy and Astrophysics* **423**(1), 13–19.
    URL: *http://adsabs.harvard.edu/abs/2004A&A...423...13N*
Ojha et al. 2012 *The Astronomer's Telegram* **4239**.
    URL: *http://adsabs.harvard.edu/abs/2012ATel.4239....1O*
Oosterbroek et al. 2008 *Astronomy and Astrophysics* **488**(1), 271–277.
    URL: *http://adsabs.harvard.edu/abs/2008A&A...488..271O*
Pacini 1967 *Nature* **216**(5115), 567–568.
    URL: *http://adsabs.harvard.edu/abs/1967Natur.216..567P*
Peng-Yoke et al. 1972 *Vistas in Astronomy* **13**(null), 1–13.
    URL: *http://dx.doi.org/10.1016/0083-6656(72)90002-5*
Petri 2012 *Monthly Notices of the Royal Astronomical Society* **424**(3), 2023–2027.
    URL: *http://mnras.oxfordjournals.org/cgi/doi/10.1111/j.1365-2966.2012.21350.x*
Popov & Stappers 2007 *Astronomy and Astrophysics* **470**(3), 1003–1007.
    URL: *http://adsabs.harvard.edu/abs/2007A&A...470.1003P*
Porth et al. 2013*a* *Monthly Notices of the Royal Astronomical Society: Letters* **431**, L48–L52.
    URL: *http://adsabs.harvard.edu/abs/2013MNRAS.431L..48P*
Porth et al. 2013*b* *Monthly Notices of the Royal Astronomical Society* **438**(1), 278–306.
    URL: *http://adsabs.harvard.edu/abs/2014MNRAS.438..278P*
Qiao et al. 2004 *The Astrophysical Journal* **606**(1), L49–L52.
    URL: *http://adsabs.harvard.edu/abs/2004ApJ...606L..49Q*
Rees & Gunn 1974 *Monthly Notices of the Royal Astronomical Society* **167**, 1–12.
    URL: *http://adsabs.harvard.edu/abs/1974MNRAS.167....1R*
Rickett & Lyne 1990 *Monthly Notices of the Royal Astronomical Society (ISSN 0035-8711)* **244**, 68–75.
    URL: *http://adsabs.harvard.edu/abs/1990MNRAS.244...68R*
Romani & Watters 2010 *The Astrophysical Journal* **714**(1), 810–824.
    URL: *http://adsabs.harvard.edu/abs/2010ApJ...714..810R*
Romani & Yadigaroglu 1995 *The Astrophysical Journal* **438**, 314.
    URL: *http://adsabs.harvard.edu/abs/1995ApJ...438..314R*
Rowan & Coontz 2004 *Science* **304**(5670), 531.
    URL: *http://www.sciencemag.org/content/304/5670/531.short*
Ruderman & Sutherland 1975 *The Astrophysical Journal* **196**, 51.
    URL: *http://adsabs.harvard.edu/abs/1975ApJ...196...51R*
Scargle 1969 *The Astrophysical Journal* **156**, 401.
    URL: *http://adsabs.harvard.edu/abs/1969ApJ...156..401S*
Schweizer et al. 2013 *Monthly Notices of the Royal Astronomical Society* **433**(4), 3325.
    URL: *http://adsabs.harvard.edu/abs/2013arXiv1301.1321S*
Shearer et al. 2003 *Science (New York, N.Y.)* **301**(5632), 493–5.
    URL: *http://adsabs.harvard.edu/abs/2003Sci...301..493S*
Shklovsky 1953 *Doklady Akademii Nauk SSSR* **90**, 983.
Sironi & Spitkovsky 2011*a* *The Astrophysical Journal* **741**(1), 39.

URL: *http://adsabs.harvard.edu/abs/2011ApJ...741...39S*

Sironi & Spitkovsky 2011*b* *The Astrophysical Journal* **726**(2), 75.
  URL: *http://adsabs.harvard.edu/abs/2011ApJ...726...75S*

Sironi et al. 2013 *The Astrophysical Journal* **771**(1), 54.
  URL: *http://iopscience.iop.org/0004-637X/771/1/54/article/*

Slowikowska et al. 2009 *Monthly Notices of the Royal Astronomical Society* **397**(1), 103–123.
  URL: *http://adsabs.harvard.edu/abs/2009MNRAS.397..103S*

Smith 2003 *Monthly Notices of the Royal Astronomical Society* **346**(3), 885–889.
  URL: *http://adsabs.harvard.edu/abs/2003MNRAS.346..885S*

Sollerman et al. 2000 *The Astrophysical Journal* **537**(2), 861–874.
  URL: *http://adsabs.harvard.edu/abs/2000ApJ...537..861S*

Spitkovsky 2006 *The Astrophysical Journal* **648**(1), L51–L54.
  URL: *http://adsabs.harvard.edu/abs/2006ApJ...648L..51S*

Strader et al. 2013 *The Astrophysical Journal Letters* **779**(1), L12.
  URL: *http://adsabs.harvard.edu/abs/2013arXiv1309.3270S*

Striani et al. 2011 *The Astrophysical Journal* **741**(1), L5.
  URL: *http://adsabs.harvard.edu/abs/2011ApJ...741L...5S*

Striani et al. 2013 *The Astrophysical Journal* **765**(1), 52.
  URL: *http://adsabs.harvard.edu/abs/2013ApJ...765...52S*

Sturrock 1971 *The Astrophysical Journal* **164**, 529.
  URL: *http://adsabs.harvard.edu/abs/1971ApJ...164..529S*

Sturrock & Aschwanden 2012 *The Astrophysical Journal* **751**(2), L32.
  URL: *http://adsabs.harvard.edu/abs/2012ApJ...751L..32S*

Tavani et al. 2011 *Science (New York, N.Y.)* **331**(6018), 736–9.
  URL: *http://adsabs.harvard.edu/abs/2011Sci...331..736T*

Tchekhovskoy et al. 2013 *Monthly Notices of the Royal Astronomical Society: Letters* **435**, L1–L5.
  URL: *http://adsabs.harvard.edu/abs/2013MNRAS.435L...1T*

Temim et al. 2006 *The Astronomical Journal* **132**(4), 1610–1623.
  URL: *http://adsabs.harvard.edu/abs/2006AJ....132.1610T*

Teraki & Takahara 2013 *The Astrophysical Journal* **763**(2), 131.
  URL: *http://adsabs.harvard.edu/abs/2013ApJ...763..131T*

Thompson et al. 1999 *The Astrophysical Journal* **516**(1), 297–306.
  URL: *http://adsabs.harvard.edu/abs/1999ApJ...516..297T*

Torres et al. 2013 *Monthly Notices of the Royal Astronomical Society* **436**(4), 3112.
  URL: *http://adsabs.harvard.edu/abs/2013arXiv1309.5291T*

Trimble 1973 *Publications of the Astronomical Society of the Pacific* **85**, 579.
  URL: *http://adsabs.harvard.edu/abs/1973PASP...85..579T*

Tziamtzis et al. 2009 *Astronomy and Astrophysics* **508**(1), 221–228.
  URL: *http://dx.doi.org/10.1051/0004-6361/200912031*

Uzdensky et al. 2011 *The Astrophysical Journal* **737**(2), L40.
  URL: *http://adsabs.harvard.edu/abs/2011ApJ...737L..40U*

Veron-Cetty & Woltjer 1993 *Astronomy and Astrophysics (ISSN 0004-6361)* **270**, 370–378.
  URL: *http://adsabs.harvard.edu/abs/1993A&A...270..370V*

Vinyaikin 2007 *Astronomy Reports* **51**(7), 570–576.
  URL: *http://adsabs.harvard.edu/abs/2007ARep...51..570V*

Vittorini et al. 2011 *The Astrophysical Journal* **732**(2), L22.
  URL: *http://adsabs.harvard.edu/abs/2011ApJ...732L..22V*

Volpi et al. 2008 *Astronomy and Astrophysics* **485**(2), 337–349.
  URL: *http://adsabs.harvard.edu/abs/2008A&A...485..337V*

Volpi et al. 2009 *eprint* **0903.4120**.
  URL: *http://adsabs.harvard.edu/abs/2009arXiv0903.4120V*

Wang et al. 2012 *Astrophysics and Space Science* **340**(2), 307–315.
    URL: *http://adsabs.harvard.edu/abs/2012Ap&SS.340..307W*
Weisskopf et al. 2000 *The Astrophysical Journal* **536**(2), L81–L84.
    URL: *http://adsabs.harvard.edu/abs/2000ApJ...536L..81W*
Weisskopf et al. 2013 *The Astrophysical Journal* **765**(1), 56.
    URL: *http://iopscience.iop.org/0004-637X/765/1/56/article/*
Weisskopf et al. 1978 *The Astrophysical Journal* **220**, L117.
    URL: *http://adsabs.harvard.edu/abs/1978ApJ...220L.117W*
Willingale et al. 2001 *Astronomy and Astrophysics* **365**(1), L212–L217.
    URL: *http://adsabs.harvard.edu/abs/2001A&A...365L.212W*
Wilson-Hodge et al. 2011 *The Astrophysical Journal* **727**(2), L40.
    URL: *http://adsabs.harvard.edu/abs/2011ApJ...727L..40W*
Wilson 1974 *Monthly Notices of the Royal Astronomical Society* **166**, 617–632.
    URL: *http://adsabs.harvard.edu/abs/1974MNRAS.166..617W*
Yuan et al. 2011 *The Astrophysical Journal* **730**(2), L15.
    URL: *http://adsabs.harvard.edu/abs/2011ApJ...730L..15Y*
Zweibel & Yamada 2009 *Annual Review of Astronomy and Astrophysics* **47**(1), 291–332.
    URL: *http://www.annualreviews.org/doi/abs/10.1146/annurev-astro-082708-101726*